International Journal of Geo-Information

MDPI

Article

Spatial Pattern Consistency among Different Remote-Sensing Land Cover Datasets: A Case Study in Northern Laos

Junmei Kang [1], Lichun Sui [1], Xiaomei Yang [2,3], Zhihua Wang [2,*], Chong Huang [2] and Jun Wang [1]

[1] Geological Engineering and Institute of Surveying and Mapping, Chang'an University, Shaanxi 710054, China; 2017026008@chd.edu.cn (J.K.); sui1011@chd.edu.cn (L.S.); 2017026007@chd.edu.cn (J.W.)

[2] State Key Laboratory of Resources and Environment Information System, Institute of Geographic Sciences and Natural Resources Research, CAS, Beijing 100101, China; yangxm@lreis.ac.cn (X.Y.); huangch@lreis.ac.cn (C.H.)

[3] Jiangsu Center for Collaborative Innovation in Geographical Information Resource Development and Application, Nanjing 210023, China

* Correspondence: zhwang@lreis.ac.cn; Tel.: +86-1861-130-1918

Received: 7 February 2019; Accepted: 29 April 2019; Published: 1 May 2019

Abstract: Comparisons of the accuracy and consistency of different remote-sensing land cover datasets are important for the rational application of multi-source land cover datasets to regional development, or to studies of global or local environmental change. Existing comparisons of accuracy or spatial consistency among land cover datasets primarily use confusion or transfer matrices and focus on the type and area consistency of land cover. However, less attention has been paid to the consistency of spatial patterns, and quantitative analyses of spatial pattern consistency are rare. However, when proportions of land cover types are similar, spatial patterns are essential for studies of the ecological functions of a landscape system. In this study, we used classical landscape indices that quantifies spatial patterns to analyze the spatial pattern consistency among different land cover datasets, and chose three datasets (GlobeLand30-2010, FROM-GLC2010, and SERVIR MEKONG2010) in northern Laos as a case study. We also analyzed spatial pattern consistency at different scales after comparing the landscape indices method with the confusion matrix method. We found that the degree of consistency between GlobeLand30-2010 and SERVIR MEKONG2010 was higher than that of GlobeLand30-2010 and FROM-GLC2010, FROM-GLC2010, and SERVIR MEKONG2010 based on the confusion matrix, mainly because of the best forest consistency and then water. However, the spatial consistency results of the landscape indices analysis show that the three datasets have large differences in the number of patches (NP), patch density (PD), and landscape shape index (LSI) at the original scale of 30 m, and decrease with the increase of the scale. Meanwhile, the aggregation index (AI) shows different changes, such as the changing trend of the forest aggregation index increasing with the scale. Our results suggested that, when using or producing land cover datasets, it is necessary not only to ensure the consistency of landscape types and areas, but also to ensure that differences among spatial patterns are minimized, especially those exacerbated by scale. Attention to these factors will avoid larger deviations and even erroneous conclusions from these data products.

Keywords: land cover products; spatial pattern; landscape index; scale; northern Laos

1. Introduction

Land cover change is closely related to global environmental change, human survival, material circulation, and global ecosystem energy cycles [1–4]. Global and regional land cover data are vital for studies of terrestrial surface processes across many research areas, including environmental monitoring,

resource surveys, biodiversity assessments, and climate change [5–7]. As remote sensing, GIS, and other technologies have become increasingly well-developed, several new global and regional land cover datasets, based on remote sensing images from multiple sources, have been released. Currently, more than 20 land cover datasets are available [8]. The most commonly used datasets are IGBP DISCOVER, produced by the US geological survey [9]; GLC2000, produced by the European union joint research center [10]; MODIS, produced by Boston University [11]; GLOBCOVER, produced by the European space agency [12,13]; LandLand30, produced by the national geomatics center of China [14]; FROM-GLC, produced by Tsinghua University [15]; and SERVIR MEKONG, produced jointly by several teams, including the United States agency for international development (USAID), the national aeronautics and space administration (NASA), and the Asian disaster preparedness center (ADPC) data. As these land cover datasets have different classification systems, classification methods, production processes, and spatial resolutions, they yield different results when applied to research questions at regional or global scales. These differences affect the use of these datasets in various fields [16,17]. Therefore, it is necessary to analyze the accuracy and consistency of these multi-source remote sensing land cover datasets in order to provide a reference for the effective use of land cover data in environmental monitoring studies.

Previous studies have assessed the accuracy and consistency of various multi-source remote sensing land cover datasets at regional or global scales [18–20]. Giri et al. [21] analyzed the degree of congruence between MODIS and GLC2000 using area consistency and the confusion matrix method. It was shown that, except for savannas, shrublands, and wetlands, data for other gross land types were generally consistent; however, in more detailed land cover categories, the degree of inconsistency increased. Mccallum et al. [22] analyzed the percentage of type area and spatial distribution consistency of four commonly used, 1-km-resolution land cover datasets on a global scale and selected seven regional scales. In this analysis, spatial distribution consistency at each location was assessed based on a four point scale: completely consistent (all four products identified the same land cover types), highly consistent (three products identified the same land cover types), consistent (two products identified the same land cover types), and completely inconsistent (all four products identified different land cover types). The results show that the spatial distribution consistency across the four data sets was limited. Using the area comparison and confusion matrix analysis methods, Tchuente et al. [23] compared the accuracy of the GLC2000, GLOBCOVER, MODIS, and ECOCLIMAP datasets on the African continent; the results showed that the consistency percent among the four land cover products was 56–69%. Focusing on the impacts of climate and altitude, Hua et al. [24] compared the spatial consistency of five land cover datasets at global and continental scales using compositional similarity, a confusion matrix, and spatial consistency analysis; it was shown that the global overall consistency of the data sets was 49.2–67.63%. Yang et al. [25] compared the accuracy of nine land cover maps of China, based on seven global land cover datasets, and found significant differences exist in land area and spatial patterns.

These studies focused on the land cover types and area consistency, and the methods they used are based on the confusion matrix which has neglect the spatial pattern information, such as the size and the shape of the connected patches. However, when the proportions of land cover types are similar, the spatial pattern information is also critical to the ecological function of the landscape system [26,27]. For example, the single large or several small reserves problem in landscape ecology queries whether species diversity is better preserved by one large reserve or by several small reserves when the total protected area is equivalent [28]. Using identical data sources and methods, Sertel et al. [29] generated three land cover maps (primary, secondary, and tertiary) and then used landscape indices analysis to compare the landscape fineness to the landscape indices. It was shown that the finer the land cover data, the more accurately the landscape features were defined. However, to our knowledge, no previous studies have specifically focused on the consistency of spatial patterns across different land cover datasets produced from different data sources or by different methods.

To compare spatial pattern consistency among different land cover datasets, we herein used classical landscape indices, which quantifies spatial distributions in landscape ecology, and then conduct

quantitative contrast experiments. Using northern Laos as a case study area, we quantitatively compare spatial pattern consistency among three high-resolution land cover datasets (GlobeLand30-2010, FROM-GLC2010, and SERVIR MEKONG2010). Since spatial distribution is still heavily dependent on spatial scale, we also experimentally compare and analyze spatial pattern consistency at different scales.

2. Study Area and Data Source

2.1. Study Area

Laos, which is a landlocked country located in the northern part of the Indo-Chinese peninsula (between 100°05–107°38′ E and 13°54′–22°30′), has an area of 236,800 km^2. Laos is bordered by the western Yunnan Plateau (Yunnan, China) to the north; by Vietnam to the east; by Thailand to the west; by Myanmar to the northwest; and by Cambodia to the south. Northern Laos is connected by the Mekong River, Asia's most important transnational water system. The land cover research in Northern Laos has important implications for ecosystem productivity, biodiversity, and biogeochemical cycles in the Mekong River Basin. Our study area included nine first-level administrative districts, including the provinces Phôngsali, Luang Namtha, Oudômxai, and Vientiane (Figure 1). The elevation of Laos is higher in the north and lower in the south; the country is inclined to the southeast in the northwest. Xiangkhoang is the highest province in Laos, with an average elevation of 1200 m. Laos has a tropical and subtropical monsoon climate, with a dry season (November–April) and a rainy season (May–October). During the rainy season, the average temperature is 24.2 °C, the average annual rainfall is about 1700 mm, and the rainfall on the plateau and mountains is about 1300 mm. During the dry season, the average temperature is 27.3 °C and there is almost no rainfall due to the dry, cool northeast wind. The little industry in the study area is primarily wood processing, rice milling, and tin mining. The main crops of Laos include rice, coffee, tobacco, and cotton.

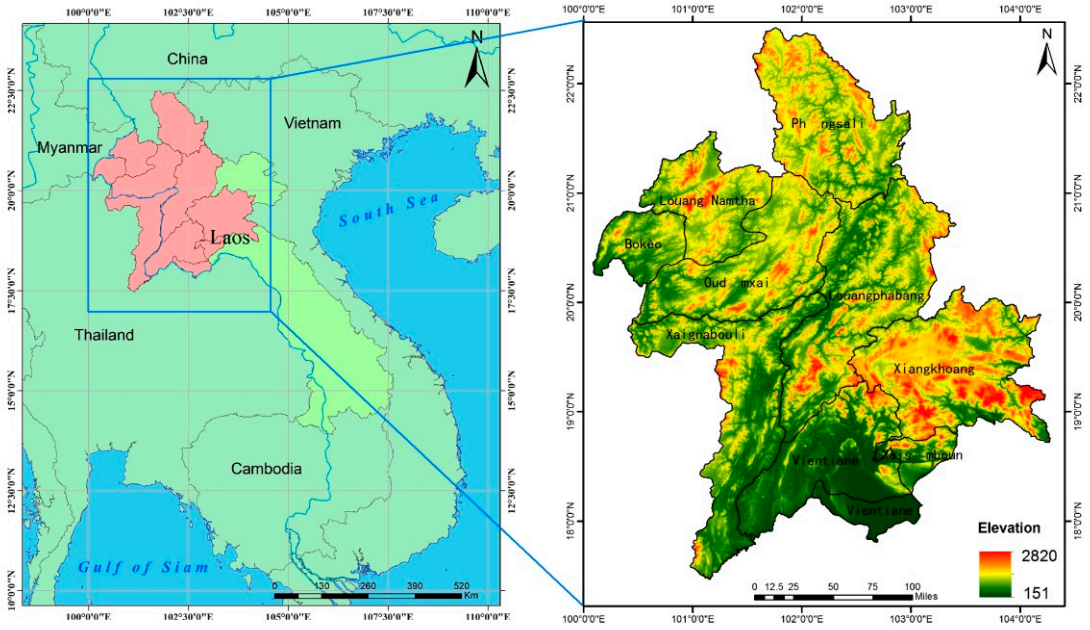

Figure 1. Location and topographic map of the study area.

2.2. Formatting of Mathematical Components

To compare spatial patterns in northern Laos, we used three global and regional land cover datasets: GlobeLand30-2010, produced by the national geomatics center of China (http://www.globallandcover.com/); FROM-GLC2010, produced by Tsinghua University, China (http://data.ess.tsinghua.edu.cn/); and the regional-scale MEKONG2010 dataset, produced by USAID, NASA, and other teams (https://rlcms-servir.adpc.net/en/landcover/); the main parameters of each dataset are summarized in Table 1.

These datasets were selected because they all have 30 m resolution and were produced in the same year. Since spatial distribution is still heavily dependent on spatial scale, it is necessary to analyze them in a multiscale way (For more details, please refer to the Section 3.3).

Table 1. Main parameters of three kinds of land cover products.

Product Name	Spatial Resolution (m)	Year	Number of Categories	Classification Technique	Overall Accuracy (%)	Publication Organization	Sensor	Coverage Area
GlobeLand30-2010	30	2010	10	POK (based on pixels, objects, and knowledge rules)	80.30	National Geomatics Center of China	Landsat TM, ETM+, HJ-1A/B	Global
FROM-GLC2010	30	2010	10 (first-class)	Support vector machine	64.90	Tsinghua University	Landsat TM/ETM+	Global
SERVIR MEKONG2010	30	2010	22	Support vector machine and random forest	Unpublished	USAID, NASA, ADPC	Landsat TM/ETM+	Indochina Peninsula

2.3. Data Preprocessing

To compare the consistency of the three datasets, we preprocessed the original data by removing all of the extraneous data (selecting only the study area), converting the projections, and merging the classification systems. We used ArcGIS software to trim the datasets and to generate new datasets with consistent boundaries (i.e., those of the study area). We used the universal transverse mercator (UTM) projection and the world geodetic system-1984 (WGS84) coordinate system.

The use of a classification system is critical for global and regional land cover mapping. Various land cover classification systems have been proposed, based on the ability of remote sensing to acquire the attributes of surface features [30–32]. In order to compare different land cover datasets, we required a unified classification system. As the classification systems used by the three land cover data sets were different, the formulations of the relevant standards were not uniform, and errors or inaccuracies may occur if there is no general category correspondence rule for direct comparisons [33]. Therefore, we standardized the code used for each land cover type across the three datasets and merged the individual sets of land cover types to establish a unified classification system. The relationship between the original classification (Table 2) and the unified system is shown in Table 3. Importantly, the classification system used by the GlobeLand30-2010 dataset (i.e., only 10 types of first-class categories) was simpler than the other two classification systems. Therefore, we reduced the complexity of the other two systems to the GlobeLand30-2010 system. Other types of merges were performed according to the GlobeLand30-2010 type definition. In addition, there were cloud coverage areas in the SERVIR MEKONG2010 data, so we remove the area data before merging the types, and other products did not consider the grid, and the final results do not include the grid in the evaluation. The three preprocessed land cover products are shown in Figure 2.

Table 2. The original classification systems of the three land cover datasets, along with the relevant codes.

Code	GlobeLand30-2010	Code	FROM-GLC2010	Code	SERVIR MEKONG2010
10	Cropland	11	Rice fields	0	Other
20	Forest	12	Greenhouse farming	1	Surface water
30	Grassland	13	Other croplands	2	Snow and Ice
40	Shrubland	21	Broadleaf forests	3	Mangrove
50	Wetland	22	Needleleaf forests	4	Flooded Forest
60	Water bodies	23	Mixed forests	5	Deciduous Forest
70	Tundra	24	Orchards	6	Orchard or Plantation Forest
80	Artificial surfaces	31	Pastures	7	Evergreen Broadleaf Alpine
90	Bareland	32	Other grasslands	8	Evergreen Broadleaf
100	Permanent snow and ice	40	Shrublands	9	Evergreen Needleleaf
		51	Marshland	10	Evergreen Mixed Forest
		52	Mudflats	11	Mixed Evergreen and Deciduous
		61	Lake	12	Urban and Built Up
		62	Reservoir/pond	13	Cropland
		63	River	14	Rice Paddy
		64	Ocean	15	Mudflat and Intertidal
		71	Shrub and Brush Tundra	16	Mining
		72	Herbaceous Tundra	17	Barren
		81	Impervious-high albedo	18	Wetlands
		82	Impervious-low albedo	19	Grassland
		91	Dry salt flats	20	Shrubland
		92	Sandy areas		
		93	Bare exposed rock		
		94	Bare herbaceous croplands		
		95	Dry lake/river bottoms		
		96	Other barren lands		
		101	Snow		
		102	Ice		
		120	Cloud		

Table 3. Types of land cover included in the study area.

Class Name	GlobeLand30-2010	FROM-GLC 2010	SERVIR MEKONG2010
1 Cropland	10	11, 12, 13	13, 14
2 Forest	20	21, 22, 23, 24	5, 8, 9, 10, 11
3 Shrubland	40	40	-
4 Grassland	30	32	-
5 Wetland	50	51, 52	4
6 Water bodies	60	61, 62, 63, 64	1
7 Artificial surfaces	80	81, 82	12
8 Bareland	90	91, 92, 93, 94, 95, 96	17
9 Others	-	101	0

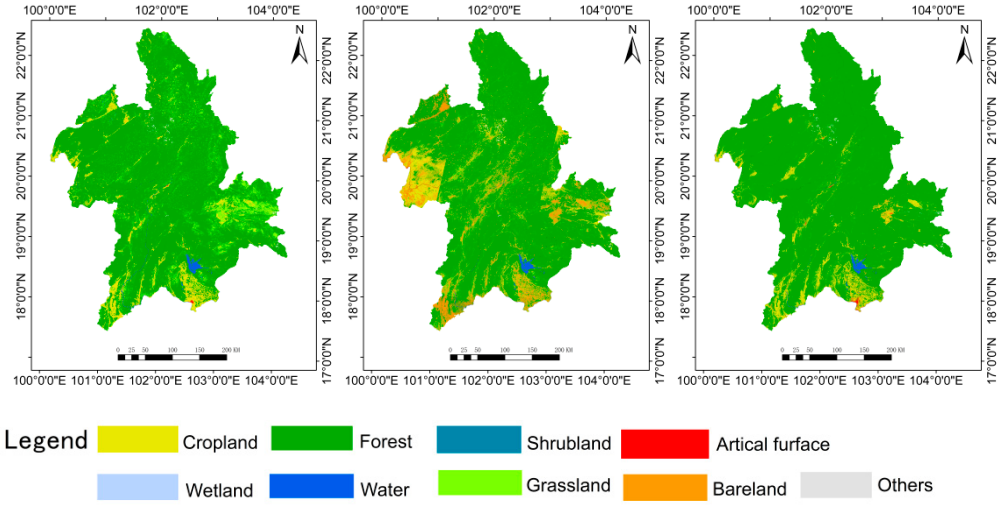

Figure 2. Three land cover products of the study area. The data from left to right are Globeland30-2010, FROM-GLC2010, and SERVIR MEKONG2010.

3. Methods

3.1. Analysis Based on Confusion Matrix and Spatial Overlay

In order to describe the consistency or confusion degree of the same land cover type among different products, every two of three remote sensing land cover products were selected, and their error matrices were calculated to obtain the consistency and confusion degree [34]. The metrics derived from error matrix are: overall accuracy, producer accuracy, and user accuracy. The calculation formulas are:

$$\mathrm{OA} = \frac{\sum_{i=1}^{8} x_{ii}}{n^2} \times 100\% \quad (1)$$

$$\mathrm{PA} = \frac{x_{ii}}{x_{+i}} \times 100\% \quad (2)$$

$$\mathrm{UA} = \frac{x_{ii}}{x_{i+}} \times 100\% \quad (3)$$

where x_{ii} is the pixel number of correctly classified of type i; n is the total number of pixels in the study area; x_{i+} is the total number of pixels of type i in the data to be verified; x_{+i} is the total number of pixels of type i in the reference data.

To determine the consistency in land cover types between the three datasets, the land cover assumed at each pixel was compared and classified as either completely inconsistent (no agreement in land cover type), basically consistent (some agreement in land cover type), or completely consistent (all datasets agree on land cover type). These results were then aggregated to determine the proportion of the study region represented by these three classes of spatial consistency.

3.2. Selection of Landscape Pattern Indices

A landscape pattern is the concrete manifestation of landscape heterogeneity, and is the result of various ecological processes acting on different scales [35,36]. The landscape pattern indices are vital for quantifying and analyzing landscape patterns, dynamic changes in landscape patterns, and the factors driving land cover composition [37–40]. At present, the number of landscape pattern indices, and the diversity of those indices, are increasing. As a single index cannot accurately reflect the real characteristics of a landscape, two or more representative indices should be used to analyze patterns and changes in the landscape. Due to the relative complexity of regional landscapes and the correlation between different landscape pattern indices, some redundancy or similarity appears in the selection

of landscape pattern indices. Thus, these indices may not fully reflect the spatial heterogeneity and diversity of the landscape. Therefore, it is necessary to understand the ecological significance of each landscape pattern index, as well as the landscape structure prerequisites that are required for use. Based on previous studies [41,42] and the characteristics of the study area, we selected the number of patches (NP) as the representative index of landscape or habitat fragmentation; patch density (PD) as the representative index of landscape spatial heterogeneity; the landscape shape index (LSI) as the representative index of shape complexity; and the aggregation index (AI) as the representative index of patch connectivity. Each index was calculated using the software Fragstats version 4.2 [43] based on eight domain rules [44]. The definition of landscape indices and their ecological significance are given in Table 4.

Table 4. Definition and ecological significance of each landscape index.

Name	Description	Ecological Significance
the number of patches (NP)	NP represents the total number of patches in the landscape $NP \geq 1$, No Upper Limit	NP is often used to describe the heterogeneity of the whole landscape. The value of NP is positively correlated with the fragmentation of the landscape. If NP is large, then landscape fragmentation is high; if NP is small, then landscape fragmentation is low.
patch density (PD)	Formula: $PD = M/A$ where N is the total number of patches, and A is the total area of the landscape PD represents the number of patches per square kilometer $PD > 0$, No Upper Limit	PD is often used to describe the degree of spatial heterogeneity and fragmentation of the landscape patches. Larger PD values imply spatial patch heterogeneity and patch fragmentation.
landscape shape index (LSI)	Formula: $LSI = \frac{0.25E}{\sqrt{A}}$ where E is the total length of all patch boundaries in the landscape, and A is the total area of the landscape $LSI \geq 1$, No Upper Limit	LSI reflects the complexity of landscape shape. As LSI approaches 1, the overall landscape shape becomes increasingly simple. When LSI = 1, there is only one patch of this type in the landscape, which is square or close to square. As LSI increases, the more complex the boundary shapes of the landscape patches are.
aggregation index (AI)	Formula: $AI = \left[\frac{g_{ij}}{\max g_{ij}}\right] \times 100$ Represents the number of pixel nodes of the patch type divided by the maximum number of nodes when the patch type is first aggregated $0 \leq AI \leq 100$	AI reflects the degree of non-randomness or aggregation of different patch types in the landscape, and shows the connectivity between patches of each landscape type. If a landscape is composed of many discrete patches, the aggregation index is low; when a few large patches dominate, or the same types of patches are highly linked, the aggregation index is high.

3.3. Multiscale Comparison of Spatial Pattern Consistence

The results of the spatial pattern analysis are heavily dependent on the spatial scale. This is a very well-known problem in spatial data analysis, called the modifiable area unit problem (MAUP), which leads to the inconsistent conclusions when the unit size and partition of the analysis are different [45]. In order to overcome the MAUP and comprehensively compare the consistency of the spatial patterns, this paper makes a comparison of the three land cover data on different spatial scales. Scaling in landscape ecology includes scaling up and scaling down. Scaling up means to move observations, tests, and simulation results from a fine scale to a larger scale [46]. Here, we focused on scaling up. We chose an appropriate scale based on previous studies [47,48]. We used ArcGIS software to resample the original land cover data using the mode sampling method, and obtained 20 different scales of land cover raster data (30, 60, 90, 120, 150, 180, 210, 240, 270, 300, 350, 400, 450, 500, 550, 600, 700, 800, 900, and 1000 m).

4. Results

4.1. Consistency by Confusion Matrix and Overlap

We selected two of the three types of land cover products as the reference data and the other product as the data needing evaluation and calculated the confusion matrix. Considering that the

error matrix values calculated by any two kinds of data reference data and the data exchange role to be evaluated are the same for consistency analysis, we only calculated the confusion matrix once for any two data. Tables 5–7 are the confusion matrices calculated by treating FROM-GLC2010, SERVIR MEKONG2010, and Globeland30-2010 as reference data, and Globeland30-2010, FROM-GLC2010, and SERVIR MEKONG2010 as corresponding data to be evaluated. The experimental results show that Globeland30-2010 and SERVIR MEKONG2010 have the highest overall consistency among land cover data, while Globeland30-2010 and FROM-GLC2010 have the lowest overall consistency. From the comparative analysis of each type of consistency, the forest and water type consistency between the two types of land cover data is higher, and the wetland type consistency is lower. Bareland-type consistency is low between Globeland30-2010 and SERVIR MEKONG2010 land cover data. The consistency of shrub, grassland, and bareland types between Globeland30-2010 and FROM-GLC2010 data is low. The reason for the low consistency between shrubs, grasslands, wetlands, and bareland types between any two types of data is mainly because the classification systems and classification methods used in the three products are different, resulting in the three products being produced on the target recognition. The huge difference is followed by the ambiguity in the classification of shrubs, woodlands, grasslands, and bareland, which also leads to large differences in the recognition of different products in remote sensing.

Table 5. Confusion matrix of FROM-GLC2010 and Globeland30-2010 (FROM-GLC2010 is reference data, Globeland30-2010 is data to be evaluated).

Type	Cropland	Forest	Shrubland	Grassland	Wetland	Water	Artificial Surface	Bareland	UA(%)
Cropland	1058717	1401589	62764	1084150	16	34234	16890	4353623	13.21
Forest	8942091	88234364	500582	3767133	17	119304	33039	4843837	82.86
Shrubland	37355	287980	732	8307	0	4701	306	42015	0.19
Grassland	1178850	8414868	116852	1570088	4	45092	6932	2066832	11.71
Wetland	939	22	1	45	0	796	149	2929	0
Water	88248	53309	1252	6144	1	728583	9662	120511	71.84
Artificial surface	8870	9027	91	3530	0	490	1333	48237	1.86
Bareland	23	390	1	24	0	1	0	64	12.65
PA(%)	9.34	89.65	0.11	24.38	0	77.77	1.94	0	
OA(%)					86.01				

Table 6. Confusion matrix of SERVIR MEKONG2010 and FROM-GLC2010 (SERVIR MEKONG2010 is reference data, FROM-GLC2010 is data to be evaluated).

Type	Cropland	Forest	Wetland	Water	Artificial Surface	Bareland	UA(%)
Cropland	1312597	9888715	1972	57017	45231	9492	11.58
Forest	2251914	96065657	1539	12466	35050	32910	97.61
Wetland	10	26	0	2	0	0	0
Water	86263	76827	2864	765891	1373	107	81.75
Artificial surface	25872	33915	88	4273	4078	97	5.94
Bareland	4759383	6291827	1981	46674	237569	140384	1.22
PA(%)	15.55	85.46	0	85.71	1.26	76.69	
OA(%)				90.88			

Table 7. Confusion matrix of Globeland30-2010 and SERVIR MEKONG2010 (Globeland30-2010 is reference data, SERVIR MEKONG2010 is data to be evaluated).

Type	Cropland	Forest	Wetland	Water	Artificial surface	Bareland	UA(%)
Cropland	4842548	3612715	3152	179575	15866	7	55.94
Forest	2805798	102690694	325	101461	11259	496	97.22
Wetland	669	2766	9	3683	3	0	0.13
Water	47139	71924	1137	722098	482	0	85.25
Artificial surface	219344	36703	279	3277	43231	0	14.27
Bareland	97610	57402	0	292	759	0	0
PA(%)	60.42	96.43	0.18	71.2	60.37	0	
OA(%)				97.15			

Based on the confusion matrix in Tables 5–7, the area consistency of the three land cover data was compared and analyzed. The three land cover data show that the forest areas account for the largest proportion. For other types, the water area consistency of the three land cover data is the highest, accounting for 0.7% of the total area of the study area. The types with large differences are shrublands, grasslands, wetlands, and bareland. SERVIR MEKONG2010 data fail to identify shrublands and grasslands in the study area. The grassland area in Globeland30-2010 is about twice that of FROM-GLC2010, and this difference in shrubland is opposite. The percentage of bareland in Globeland30-2010 is only 0.0005%, while the bareland in FROM-GLC2010 accounts for up to 8.81%. For the wetland type, Globeland30-2010 and SERVIR MEKONG2010 have good data consistency, and the area ratio is 0.003% and 0.006%, respectively.

In order to facilitate the visual analysis of the spatially consistent distribution characteristics of multi-source land cover remote sensing data, the three products are spatially superimposed in Figure 3. The results show that the complete spatial consistency area accounts for 67.83% of the total area of the study area. The northern, central, southeastern, and northwestern areas of the study area are distributed, mainly because of the pattern of forest dominating, and water and cropland being relatively less in the study area. So, the land cover type in the completely consistent area is relatively simple, and the spectral features are simple or express the obvious phenological characteristics. The distribution of the basic consistent areas, accounting for 26.54% of the total area of the study area, conforms to the regional variable characteristics of the land cover category, which is mainly located around the completely consistent area. It is mainly distributed in the southern and western parts of the study area and few in the central and eastern parts. The land cover types in these areas are mainly cropland and forest. The area of the inconsistent area accounts for 5.63% of the total area of the study area, mainly distributed in the eastern, southern, and central areas of the study area. The land cover types in these areas are more complex, and the land surface types show obvious heterogeneity characteristics, and cropland, forest, shrubland, grassland, and bareland are staggered.

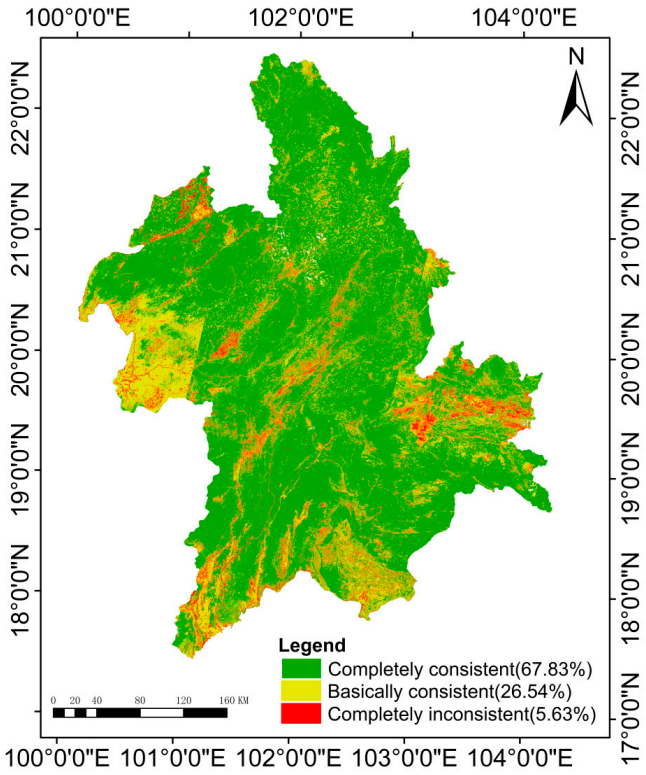

Figure 3. Spatial consistency maps of three land cover data. The percent numbers in the legend are the area proportion of each component.

4.2. Spatial Pattern Consistency Analysis Based on Landscape Indices at the Original Scale

We determined the landscape indices values for each type of land cover in the study area based on each dataset (Table 6). There were some differences in the spatial patterns of croplands across the three datasets. The NP, PD, and LSI values calculated using the FROM-GLC2010 dataset were the highest across all three datasets, while the AI value was the lowest. This indicated that the FROM-GLC2010 data identified more cropland fragmentation and spatial patch heterogeneity. In the FROM-GLC2010 data, patch shapes were more complicated, and the degree of aggregation between the patches was low. In the Globeland30-2010 data, the cropland landscape was not highly fragmented, the patch shapes were simple, and the patches were highly connected. Therefore, the Globeland30-2010 and SERVIR MEKONG2010 datasets were similar with respect to cropland identification.

More than 70% of northern of Laos is forest land, and this was the main type of land cover in the study area. All three datasets showed a high degree of aggregation and patch self-similarity for forest land. However, the three datasets differed in the degree of fragmentation and shape complexity of the forest patches. The FROM-GLC2010 data suggested a high degree of fragmentation and complexity, while the SERVIR MEKONG2010 data suggested the opposite.

The FROM-GLC2010 data identified a high degree of shrubland and grassland fragmentation and spatial heterogeneity, with complex patch shapes and little aggregation between patches. This dataset suggested that shrubland in the study area were small and scattered.

Wetland landscapes accounted for less of the study area. Wetland patch fragmentation, spatial heterogeneity, and patch shape complexity were basically consistent between Globeland30-2010 and FROM-GLC2010 datasets, but patch connectivity was higher in the Globeland30-2010 datasets than in the other two data sets. The spatial patterns of water differed little among the three datasets, especially between FROM-GLC2010 and SERVIR MEKONG2010 data. The dispersion of the water landscape was low in the Globeland30-2010 dataset.

The patch fragmentation, patch shape complexity, and dispersion between patches were low for surface landscapes in the Globeland30-2010 dataset. Surface landscapes in the SERVIR MEKONG2010 dataset were the most fragmented and complex, as compared to the other two datasets, although the degree of surface landscape aggregation was higher than that of the FROM-GLC2010 dataset. The landscape indices for bareland differed greatly among datasets. The FROM-GLC2010 dataset suggested the highest patch aggregation, with high fragmentation and patch shape complexity, while the Globeland30-2010 data suggested the opposite.

4.3. Comparison of Spatial Patterns at Different Scales

Changes in the landscape scale may alter patch boundaries, divide or fuse patches, and may thus alter landscape patterns, leading to corresponding changes in the indices of these patterns [49,50]. The landscape pattern indices of each type of land cover data changed differently as the scale increased.

As the spatial scale granularity of croplands increased, NP, PD, and LSI tended to converge among datasets, but AI values differed (Figure 4). At scales of 30–60 m, NP, PD, and LSI values based on FROM-GLC2010 and SERVIR MEKONG2010 data decreased rapidly; these values decreased more slowly at scales >60 m. Scale changes had little effect on the NP, PD, and LSI values of the Globeland30-2010 data. At 60 m, the AI value of the FROM-GLC2010 and SERVIR MEKONG2010 data suddenly increased, while the AI value of three datasets show a steady decreasing trend at other scales.

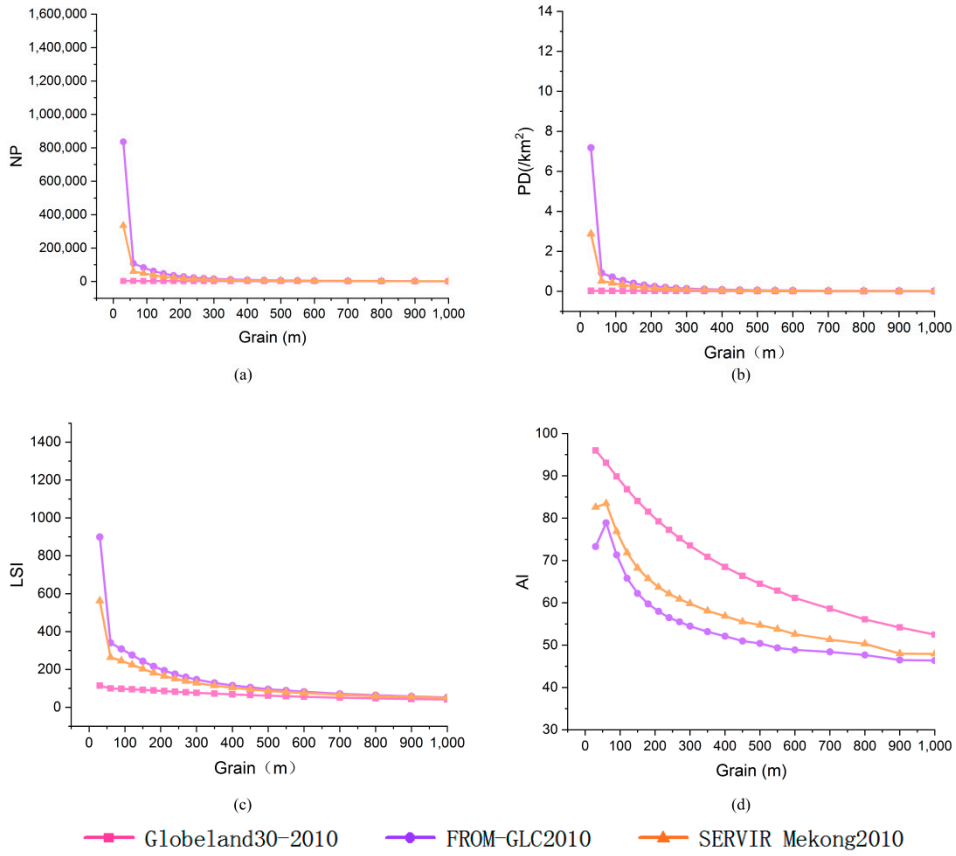

Figure 4. The cropland landscape pattern indices changing curves with scale increasing. (**a**) is the NP curve; (**b**) is the PD curve; (**c**) is the LSI curve; (**d**) is the AI curve.

The three datasets suggested that landscape pattern indices for forest lands have high consistency at increasing spatial scales (Figure 5). At a scale of 60 m, the NP, PD, and LSI values decreased sharply, while the AI value increased sharply. Similar to the cropland landscape, as the spatial scale increased, NP, PD, and LSI tended to converge across datasets, while the AI values differed.

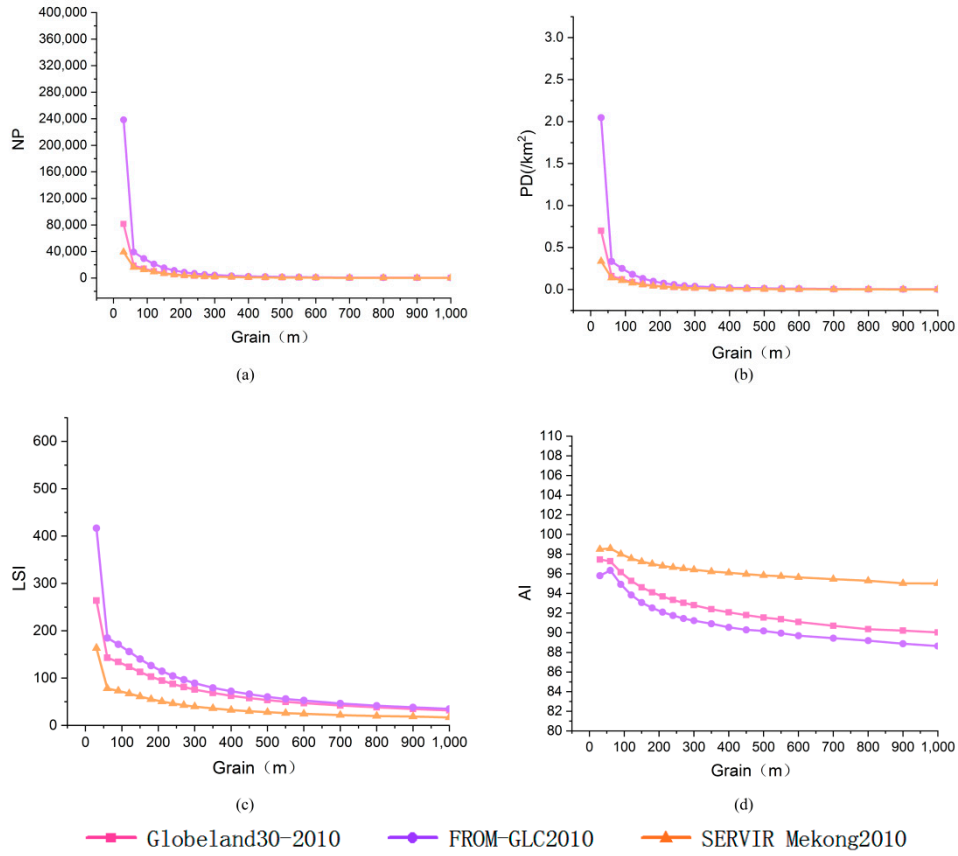

Figure 5. The forest landscape pattern indices changing curves with scale increasing. (**a**) is the NP curve; (**b**) is the PD curve; (**c**) is the LSI curve; (**d**) is the AI curve.

As scale increased, wetlands indices values differed among the three datasets (Figure 6). When the scale increased gradually, the NP and PD values for wetlands based on the FROM-GLC2010 and Globeland30-2010 datasets showed high consistency trends across all scales, and scale had only a very slight influence on the indices values. The LSI value of the three datasets showed little difference in landscape index curve with scale increasing. The effects of scale on AI showed low consistency across the three datasets, and they have different fluctuation points in the whole scale range.

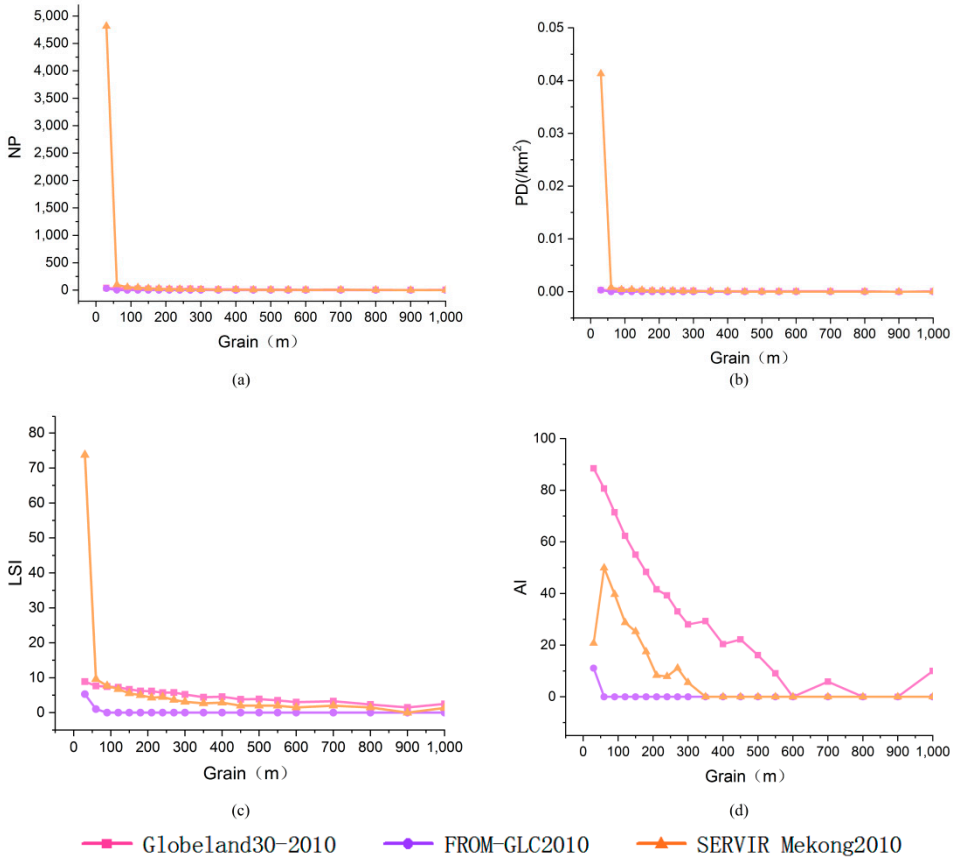

Figure 6. The wetland landscape pattern indices changing curves with scale increasing. (**a**) is the NP curve; (**b**) is the PD curve; (**c**) is the LSI curve; (**d**) is the AI curve.

The effects of scale on the water landscape pattern indices were consistent among the three datasets (Figure 7). When the scale was 60 m, the NP, PD, and LSI indices values dropped sharply, while other indices were gradually decreasing. The indices values became gradually more similar among datasets with scale increasing.

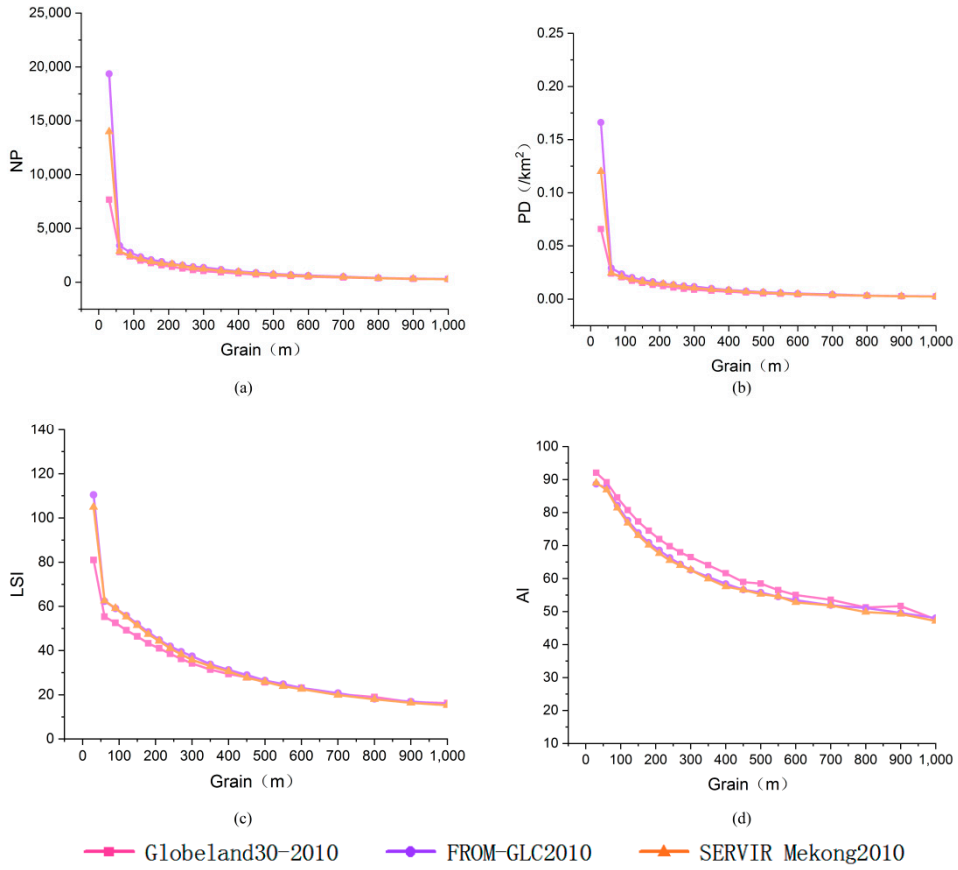

Figure 7. The water landscape pattern indices changing curves with scale increasing. (**a**) is the NP curve; (**b**) is the PD curve; (**c**) is the LSI curve; (**d**) is the AI curve.

The effects of scale on the NP, PD, and LSI indices of artificial surfaces were similar to those observed for cropland (Figure 8). The AI values of FROM-GLC2010 and SERVIR MEKONG2010 datasets increase sharply at a scale of 60 m, while the AI values decreased with slight fluctuations in other scale ranges.

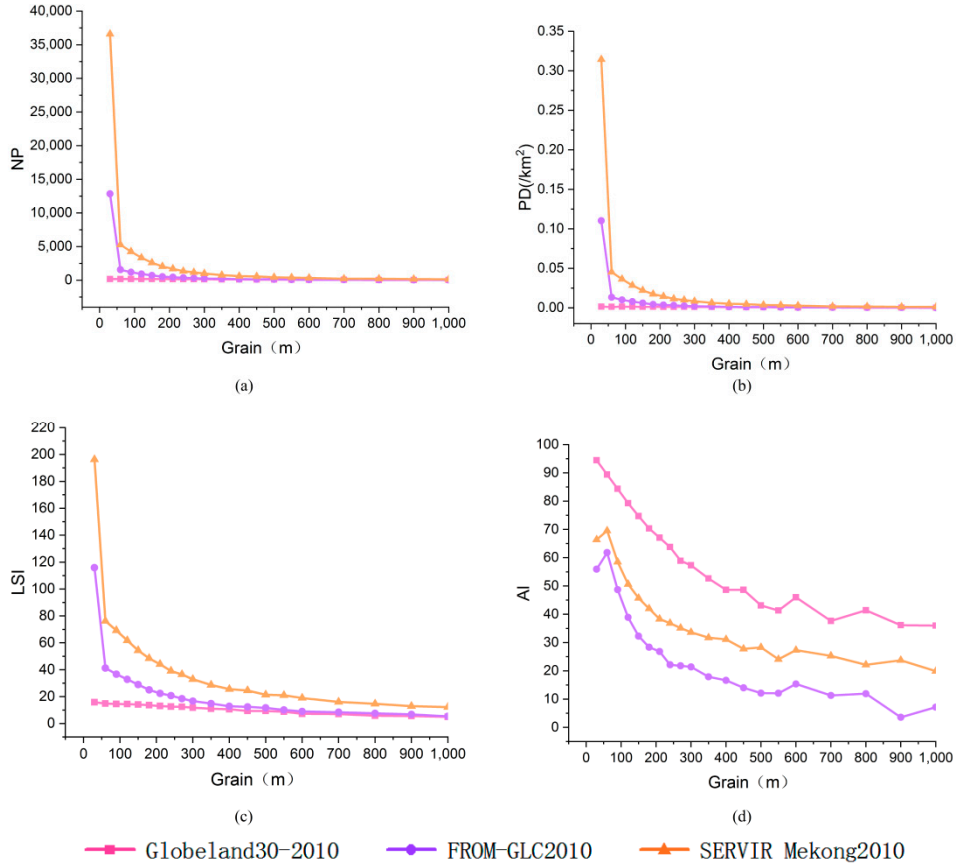

Figure 8. The artificial surface landscape indices changing curves with scale increasing. (**a**) is the NP curve; (**b**) is the PD curve; (**c**) is the LSI curve; (**d**) is the AI curve.

The increase in spatial scale affected the NP, PD, and LSI bareland indices similarly to the cropland indices across all three datasets (Figure 9). At a scale of 30–150 m, the AI values in Globe-land 30-2010 decrease rapidly and tend to be stable when the scale is larger than 150 m; The turning point of SERVIR MEKONG2010 data is 60 m, while the FROM-GLC2010 data decreases slowly in the whole scale.

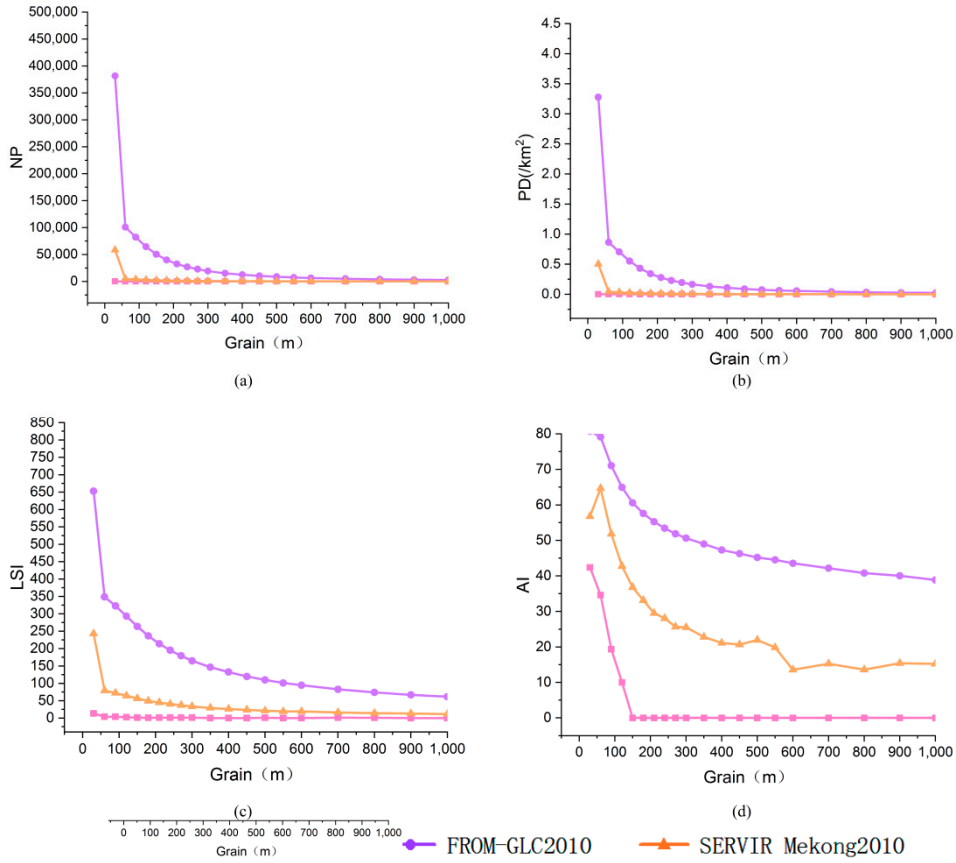

Figure 9. The bareland landscape pattern indices changing curves with scale increasing. (**a**) is the NP curve; (**b**) is the PD curve; (**c**) is the LSI curve; (**d**) is the AI curve.

5. Discussion

5.1. Consistency Analysis at the Original Dataset Scale

Confusion matrix and spatial overlay visual analysis (after normalizing the original datasets) indicated serious inconsistencies among different landscape types (i.e., forest, shrublands, grasslands, croplands, and bareland). Shrublands and grasslands were not identified by the SERVIR MEKONG2010 dataset. Although the other two datasets identified shrublands and grasslands, the consistency of this type between them was low. The primary reason for these misclassifications is that there are no obvious differences in life form, spectral, and textural characteristics among shrublands, grasslands, and forest. During the imaging process, it is easy to capture different objects with the same spectrum that are difficult to distinguish. The accuracy of the classification system also affects land cover classification [51]. For example, the vegetation coverage and tree height thresholds are not clearly defined for forests, shrublands, and grasslands in the SERVIR MEKONG2010 dataset. Therefore, this classification system may require further revision to reduce the number of fuzzy concepts used. In addition, croplands are typically distributed as concentrated sheets, shrublands are often mixed with forests and croplands. Differences in vegetation thresholds of the different datasets further aggravates the incongruence. In the future, other auxiliary data should be considered to increase the accuracy of classification. Such problems are common in optical remote-sensing classification applications with multi-temporal spectral characteristics. Therefore, it is necessary to improve the accuracy of land cover classification recognition algorithms and by introducing multi-source data and knowledge.

The above consistency analysis was mainly based on dataset generation standards, confusion matrix, and spatial overlay visual analysis. Fine-scale visual comparisons of spatial consistency are subjective. By using the landscape indices to quantify spatial distributions, many subtle differences can

be identified. For example, in the SERVIR MEKONG 2010 datasets, shrublands and grasslands were primarily identified as forest lands, leading to increases in forest land connectivity, patch closeness, and AI. Therefore, the loss of shrublands and grasslands impacts the AI of the forest landscape (as shown in Table 8), affecting ecosystem stability, biodiversity conservation, animal reproduction, and biological resource management. Data users must deliberately choose suitable land cover datasets based on research objectives and research area characteristics. The indices used here might be useful for assessing aspects of ecosystem function, including the determination of spatial distribution characteristics for various species and secondary species in the landscape, changes in the interactions among species, and the stability of synergistic symbiosis. Therefore, when selecting multi-source remote-sensing land cover datasets, researchers must not only consider the consistency of areas and qualitative spatial patterns, but also quantitative spatial pattern distribution, especially for studies of ecosystems and ecosystem functions.

Table 8. The landscape pattern characteristics of various types of land cover data.

Class Name	Dataset	NP	PD(/km^2)	LSI	AI
Cropland	G	2983	0.0256	114.4704	95.9898
	F	836,198	7.1813	899.8113	73.2971
	S	335,045	2.8772	562.8378	98.5
Forest	G	81,487	0.6998	263.8612	97.4524
	F	238,426	2.0476	416.6991	95.8093
	S	39,282	0.3373	163.4867	98.5
Shrubland	G	41,268	0.3544	206.8584	66.6069
	F	286,287	2.4586	581.6292	29.5878
	S	-	-	-	-
Grassland	G	399,254	3.4287	690.6286	81.1601
	F	624,280	5.3613	974.7675	61.6149
	S	-	-	-	-
Wetland	G	40	0.0003	8.9149	88.4842
	F	30	0.0003	5.3077	11.1111
	S	4,815	0.0413	73.7366	20.7533
Water	G	7,672	0.0659	81.0065	92.0437
	F	19,356	0.1662	110.4954	88.6749
	S	13,989	0.1201	104.936	88.9963
Artificial surface	G	176	0.0015	15.8153	94.4346
	F	12,847	0.1103	115.84	55.9537
	S	36,606	0.3145	196.337	66.3918
Bareland	G	157	0.0013	13.3778	42.3992
	F	381,621	3.2774	652.7455	80.7655
	S	58,487	0.5023	243.0855	56.7812

Note: symbol "-" indicates no data for the study area, G represents Globeland30-2010 data, F represents FROM-GLC2010 data, and S represents SERVIR MEKONG2010 data.

5.2. Consistency of Spatial Patterns at Different Scales

Scale strongly influences spatial pattern analyses [52]. By comparing the spatial patterns of the three datasets at different scales, we found that the NP, PD, and LSI indices values differed greatly at scales between 30 m and 150 m. At scales >150 m, the difference gradually decreases and eventually tends to be consistent, but there is still some difference in AI value with scale increasing. For example, in Vientiane Province (Figure 10), indices values varied greatly among datasets at 30 m, due to the different classification methods and classification systems; as scale increased gradually, small patches were integrated into large patches, decreasing the number of patches of each type, and leading to decreases in NP and PD values. Through constant fragmentation and fusion, original patch shapes

were destroyed, and new patch shapes tended to be regular. This substantially reduced LSI values. So, differences between the datasets gradually decreased. At scales greater than 150 m, the three datasets differed little in their assessments of ecosystem function, including landscape fragmentation, heterogeneity, and shape complexity. However, at scales <150 m, differences between datasets were large. Thus, the differences among datasets might strongly influence ecosystem-based landscape analyses. In addition, AI values remained incongruent among the three datasets, even at large scales, because the AI index is affected by the richness of the structural components and their spatial allocations [45]. As scale increased, the spatial allocation of new patches caused by grid cell aggregation might have led to the substantial differences in AI values observed among the three datasets. Therefore, studies of ecosystem connectivity should carefully consider the differences among datasets across all spatial scales.

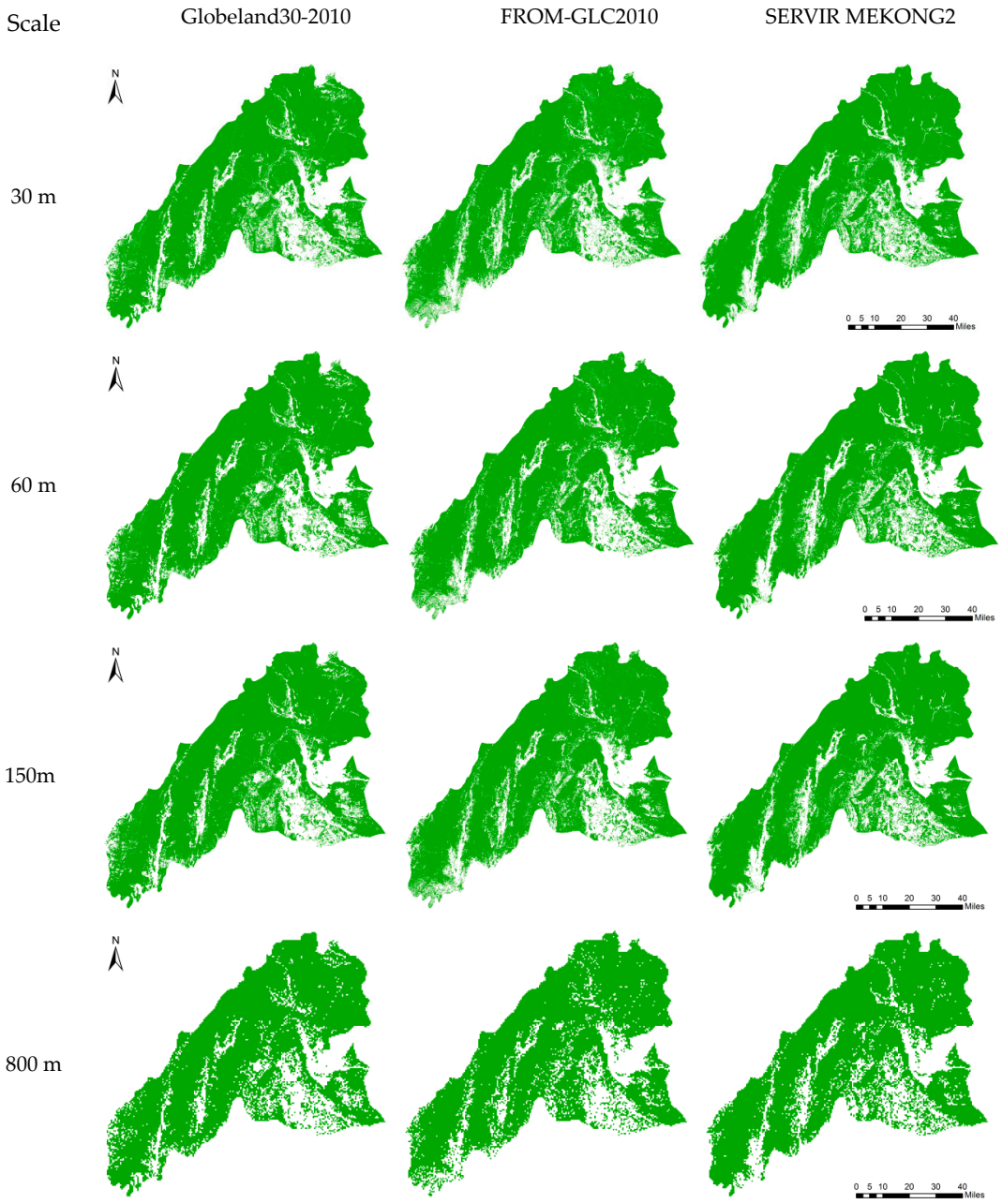

Figure 10. Spatial pattern distributions of three land cover datasets forest type at different scales.

In the comparative analysis of spatial patterns at different scales, we found that the values of landscape indices changed abruptly at certain spatial scales. The main turning point was 60 m. It was possible that, when the resolution was close to the intrinsic scale of small terrestrial patches, the number and connectivity of these patches changed substantially. As scale continued to increase, the intrinsic scale of the patch changes, and the indices gradually declines. Population dynamics, biodiversity, and ecosystems are inevitably affected by the spatial pattern of the landscape. Therefore, it is necessary to identify differences in the spatial pattern distributions captured by different datasets at different scales. Indeed, although the overall differences among landscape indices were low with scale increasing, future studies should be mindful of each of these change points.

5.3. Spatial Consistency Analysis and Absolute Accuracy Evaluation

Absolute accuracy evaluation results are of great significance for selecting and comparing different land cover products, especially when two or more products are inconsistent. It is a meaningful study to provide a standard for researchers to choose the right data. There has been a lot of research on this [25,53].

However, the study of land cover product consistency also has its scientific value. For example, when the spatial consistency of multiple sets of land cover products in a region is good, it indicates that the mapping accuracy of this area is relatively high, and these land use products can be used at a high degree; if the consistency is low, it indicates that the accuracy of mapping in this area is likely to be low. At this time, we may adopt the following suggestion of Giri et al. [21]:

"Data producers may use the areas of spatial agreement for training area selection and pay special attention to areas of disagreement for further improvement in future land cover characterization and mapping. Users can conveniently use the findings in the areas of agreement, whereas users might need to verify the information in the areas of disagreement with the help of secondary information."

The paper aims to reveal the phenomenon or fact that product consistency comparison should not only consider type or area, but also their spatial pattern. This phenomenon has not been noticed in previous studies like Hua et al. [24]. We used the landscape indices, which can quantitatively express the spatial pattern and perform a quantitative case study on the inconsistency of the spatial pattern. We believe that it is useful to study this phenomenon, because: (1) it can remind producers not only to pursue the accuracy of type and area, but also the accuracy of spatial pattern when producing data products; (2) it also reminds users that when using different land use data, they need to consider the difference of spatial pattern relating to function analysis; (3) Landscape indices can measure the spatial pattern difference, thus can be referred by both producers and users.

Besides, the landscape indices analysis method used in this study can also be applied to the absolute accuracy evaluation of different data products. More specifically, researchers can compare the landscape indices of multiple land cover data with the landscape indices of the correct reference data. The closer the indices are, the better the consistency can reach. However, to achieve this method, we need to pay attention to the following two problems: (1) it is very difficult to obtain the correct reference data covering the whole region in practice, and we need to use a statistical inference method which requires a reasonable layout of sample areas. This is completely different from the traditional layout of sample points and requires a new spatial sampling method; (2) For different types of land cover and application purposes, the focus of the spatial pattern may be different. It is necessary for researchers to select landscape indices with corresponding meanings for specific analysis according to specific purpose. However, the solutions of the above two problems need more innovative ideas and study cases.

6. Conclusions

To test the spatial pattern consistency of different land cover datasets, we herein used the quantitative landscape indices to compare the spatial pattern consistency at different spatial scales. We used three land cover datasets covering northern Laos in the same year (2010) as a case study.

Our results indicated that the relative areas identified for each landscape types were similar across the three datasets, but the recovered spatial patterns differed substantially. With the exception of AI, most of the differences among datasets decreased as spatial scale increased. However, some land types still exhibited a spatial pattern mutation. Our results indicated that, when studying ecosystem function based on landscape patterns, land cover datasets should be chosen according to the research aims. In addition, the impact of changes in spatial pattern, especially scale, requires special attention. In addition, dataset producers should evaluate the accuracy between quantity and spatial patterns. In this way, inconsistencies among datasets might be reduced, and comparability increased.

Author Contributions: Conceptualization, Zhihua Wang, Lichun Sui, Xiaomei Yang; methodology, Zhihua Wang, Lichun Sui, Chong Huang, and Junmei Kang; software, Junmei Kang and Jun Wang; validation, Junmei Kang and Chong Huang; formal analysis, Junmei Kang and Zhihua Wang; resources, Xiaomei Yang and Chong Huang; writing—original draft preparation, Junmei Kang; writing—review and editing, Zhihua Wang, Lichun Sui, and Xiaomei Yang; visualization, Junmei Kang and Jun Wang; supervision, Lichun Sui and Xiaomei Yang; project administration, Xiaomei Yang; funding acquisition, Xiaomei Yang.

Funding: This study was supported by the National Key Research and Development Program of China, Grant No. 2016YFB0501404; the CAS Earth Big Data Science Project, Grant No. XDA19060303; the National Science Foundation of China, Grant No. 41671436 and the Innovation Project of LREIS, Grant No. O88RAA01YA.

Acknowledgments: We are grateful to Fengshuo Y., Yueming L., Chen L., Bin L. (Institute of Geographic Sciences and Natural Resources Research, Chinese Academy of Sciences), and Zhi L. (Xinjiang Institute of Ecology and Geography, Chinese Academy of Sciences) for their help in method implementation, results validation and visualization, and also to Yuanzheng M. for his reviewing. Furthermore, we would like to thank the anonymous reviewers for their valuable comments.

Conflicts of Interest: The authors declare no conflict of interest.

References

1. Hereher, M.E. Effects of land use/cover change on regional land surface temperatures: Severe warming from drying Toshka lakes, the Western Desert of Egypt. *Nat. Hazards* **2017**, *88*, 1–15. [CrossRef]
2. Philpott, S.M.; Lin, B.B.; Jha, S.; Brines, S.J. A multi-scale assessment of hurricane impacts on agricultural landscapes based on land use and topographic features. *Agric. Ecosyst. Environ.* **2008**, *128*, 12–20. [CrossRef]
3. Qiu, G.-Y.; Yin, J.; Geng, S. Impact of climate and land-use changes on water security for agriculture in Northern China. *J. Integr. Agric.* **2012**, *11*, 144–150. [CrossRef]
4. Turner, B.L.; Lambin, E.F.; Anette, R. The emergence of land change science for global environmental change and sustainability. *Proc. Natl. Acad. Sci. USA* **2007**, *104*, 20666–20671. [CrossRef] [PubMed]
5. Giri, C.; Defourny, P.; Shrestha, S. Land cover characterization and mapping of continental Southeast Asia using multi-resolution satellite sensor data. *Int. J. Remote Sens.* **2003**, *24*, 4181–4196. [CrossRef]
6. Sutherland, W.J.; Adams, W.M.; Aronson, R.B.; Aveling, R.; Blackburn, T.M.; Broad, S.; Ceballos, G.; Cã´Tã, I.M.; Cowling, R.M.; Da, F.G. One hundred questions of importance to the conservation of global biological diversity. *Conserv. Biol.* **2010**, *23*, 557–567. [CrossRef]
7. Wang, Z.; Yang, X.; Chen, L.; Yang, F. A scale self-adapting segmentation approach and knowledge transfer for automatically updating land use/cover change databases using high spatial resolution images. *Int. J. Appl. Earth Obs. Geoinf.* **2018**, *69*, 88–98. [CrossRef]
8. Grekousis, G.; Mountrakis, G.; Kavouras, M. An overview of 21 global and 43 regional land-cover mapping products. *Int. J. Remote Sens.* **2015**, *36*, 1–27. [CrossRef]
9. Loveland, T.R.; Reed, B.C.; Brown, J.F.; Ohlen, D.O.; Zhu, Z.; Yang, L.; Merchant, J.W.; Defries, R.S.; Belward, A.S. Development of a global land cover characteristics database and IGBP DISCover from 1 km AVHRR data. *Int. J. Remote Sens.* **2000**, *21*, 1303–1330. [CrossRef]
10. Corresponding, E.B.; Belward, A.S. GLC2000: A new approach to global land cover mapping from earth observation data. *Int. J. Remote Sens.* **2005**, *26*, 1959–1977.
11. Friedl, M.A.; Sulla-Menashe, D.; Tan, B.; Schneider, A.; Ramankutty, N.; Sibley, A.; Huang, X. MODIS collection 5 global land cover: Algorithm refinements and characterization of new datasets. *Remote Sens. Environ.* **2010**, *114*, 168–182. [CrossRef]

12. Arino, O.; Gross, D.; Ranera, F.; Bourg, L.; Leroy, M.; Bicheron, P.; Latham, J.; Gregorio, A.D.; Brockman, C.; Witt, R. GlobCover: ESA service for global land cover from MERIS. In Proceedings of the IEEE International Geoscience & Remote Sensing Symposium, Barcelona, Spain, 23–28 July 2007.
13. Defourny, P.; Schouten, L.; Bartalev, S.; Bontemps, S.; Caccetta, P.; de Wit, A.J.W.; Di Bella, C.; Gérard, B.; Giri, C.; Gond, V.; et al. Accuracy assessment of a 300 m global land cover map: The globcover experience. In Proceedings of the 33rd International Symposium on Remote Sensing of Environment (ISRSE), Stresa, Italy, 4–8 May 2009.
14. Chen, J.; Jin, C.; Liao, A.; Xin, C.; Chen, L.; Chen, X.; He, C.; Gang, H.; Shu, P.; Miao, L. Global land cover mapping at 30 m resolution: A POK-based operational approach. *ISPRS J. Photogramm. Remote Sens.* **2015**, *103*, 7–27. [CrossRef]
15. Gong, P.; Wang, J.; Yu, L.; Zhao, Y.; Zhao, Y.; Liang, L.; Niu, Z.; Huang, X.; Fu, H.; Liu, S. Finer resolution observation and monitoring of global land cover: First mapping results with Landsat TM and ETM+ data. *Int. J. Remote Sens.* **2013**, *34*, 2607–2654. [CrossRef]
16. Congalton, R.G.; Gu, J.; Yadav, K.; Thenkabail, P.; Ozdogan, M. Global land cover mapping: A review and uncertainty analysis. *Remote Sens.* **2014**, *6*, 12070–12093. [CrossRef]
17. Tsendbazar, N.E.; Bruin, S.D.; Herold, M. Assessing global land cover reference datasets for different user communities. *ISPRS J. Photogramm. Remote Sens.* **2015**, *103*, 93–114. [CrossRef]
18. Cui, H.; Jiang, L.; Du, J.; Zhao, S.; Wang, G.; Zheng, L.; Jian, W.; Cui, H.; Jiang, L.; Du, J. Evaluation and analysis of AMSR-2, SMOS, and SMAP soil moisture products in the Genhe area of China. *J. Geophys. Res. Atmos.* **2017**, *122*, 8650–8666. [CrossRef]
19. Pflugmacher, D.; Krankina, O.N.; Cohen, W.B.; Friedl, M.A.; Sulla-Menashe, D.; Kennedy, R.E.; Nelson, P.; Loboda, T.V.; Kuemmerle, T.; Dyukarev, E.; et al. Comparison and assessment of coarse resolution land cover maps for Northern Eurasia. *Remote Sens. Environ.* **2011**, *115*, 3539–3553. [CrossRef]
20. Schultz, M.; Tsendbazar, N.E.; Herold, M.; Jung, M.; Mayaux, P.; Goehmann, H. Utilizing the global land cover 2000 reference dataset for a comparative accuracy assessment of global 1 km land cover maps. *ISPRS Arch.* **2015**, *XL-7/W3*, 503–510. [CrossRef]
21. Giri, C.; Zhu, Z.; Reed, B. A comparative analysis of the global land cover 2000 and MODIS land cover data sets. *Remote Sens. Environ.* **2005**, *94*, 123–132. [CrossRef]
22. Mccallum, I.; Obersteiner, M.; Nilsson, S.; Shvidenko, A. A spatial comparison of four satellite derived 1 km global land cover datasets. *Int. J. Appl. Earth Obs. Geoinf.* **2006**, *8*, 246–255. [CrossRef]
23. Tchuenté, A.T.K.; Roujean, J.L.; Jong, S.M.D. Comparison and relative quality assessment of the GLC2000, GLOBCOVER, MODIS and ECOCLIMAP land cover data sets at the African continental scale. *Int. J. Appl. Earth Obs. Geoinf.* **2011**, *13*, 207–219. [CrossRef]
24. Hua, T.; Zhao, W.; Liu, Y.; Wang, S.; Yang, S. Spatial consistency assessments for global land-cover datasets: A comparison among GLC2000, CCI LC, MCD12, GLOBCOVER and GLCNMO. *Remote Sens.* **2018**, *10*, 1846. [CrossRef]
25. Yang, Y.; Xiao, P.; Feng, X.; Li, H. Accuracy assessment of seven global land cover datasets over China. *ISPRS J. Photogramm. Remote Sens.* **2017**, *125*, 156–173. [CrossRef]
26. Blumstein, M.; Thompson, J.R. Land-use impacts on the quantity and configuration of ecosystem service provisioning in Massachusetts, USA. *J. Appl. Ecol.* **2015**, *52*, 1009–1019. [CrossRef]
27. Mcintyre, S. The role of plant leaf attributes in linking land use to ecosystem function in temperate grassy vegetation. *Agric. Ecosyst. Environ.* **2008**, *128*, 251–258. [CrossRef]
28. Simberloff, D. Experimental zoogeography of islands: Effects of island size. *Ecology* **1976**, *57*, 629–648. [CrossRef]
29. Sertel, E.; Topaloglu, R.H.; Salli, B.; Algan, I.Y.; Aksu, G.A. Comparison of landscape metrics for three different level land cover/land use maps. *ISPRS Int. J. Geo Inf.* **2018**, *7*, 408. [CrossRef]
30. Hansen, M.C.; Defries, R.S.; Townshend, J.R.G.; Sohlberg, R. Global land cover classification at 1 km spatial resolution using a classification tree approach. *Int. J. Remote Sens.* **2000**, *21*, 1331–1364. [CrossRef]
31. Homer, C.; Dewitz, J.; Fry, J.; Coan, M.; Hossain, N.; Larson, C.; Herold, N.; McKerrow, A.; VanDriel, J.N.; Wickham, J. Completion of the 2001 national land cover database for the conterminous United States. *Photogramm. Eng. Remote Sens.* **2007**, *73*, 337–341.
32. Zhang, J.; Feng, Z.; Jiang, L. Progress on Studies of Land Use/Land Cover Classification Systems. *Resour. Sci.* **2011**, *33*, 1195–1203.

33. Latifovic, R.; Olthof, I. Accuracy assessment using sub-pixel fractional error matrices of global land cover products derived from satellite data. *Remote Sens. Environ.* **2004**, *90*, 153–165. [CrossRef]
34. Congalton, R.G.; Green, K. *Assessing the Accuracy of Remotely Sensed Data—Principles and Practices*, 2nd ed.; CRC Press, Taylor & Francis Group: Boca Raton, FL, USA, 2009; ISBN 978-1-4200-5512-2.
35. Kedron, P.J.; Frazier, A.E.; Ovando-Montejo, G.A.; Wang, J. Surface metrics for landscape ecology: A comparison of landscape models across ecoregions and scales. *Landsc. Ecol.* **2018**, *33*, 1489–1504. [CrossRef]
36. Suárez-Castro, A.F.; Simmonds, J.S.; Mitchell, M.G.E.; Maron, M.; Rhodes, J.R. The scale-dependent role of biological traits in landscape ecology: A review. *Curr. Landsc. Ecol. Rep.* **2018**, *3*, 12–22. [CrossRef]
37. Fan, Q.; Ding, S. Landscape pattern changes at a county scale: A case study in Fengqiu, Henan Province, China from 1990 to 2013. *Catena* **2016**, *137*, 152–160. [CrossRef]
38. Sun, B.; Zhou, Q. Expressing the spatio-temporal pattern of farmland change in arid lands using landscape metrics. *J. Arid Environ.* **2016**, *124*, 118–127. [CrossRef]
39. Wan, L.; Zhang, Y.; Zhang, X.; Qi, S.; Na, X. Comparison of land use/land cover change and landscape patterns in Honghe National Nature Reserve and the surrounding Jiansanjiang Region, China. *Ecol. Indic.* **2015**, *51*, 205–214. [CrossRef]
40. Zhang, F.; Yushanjiang, A.; Wang, D. Ecological risk assessment due to land use/cover changes (LUCC) in Jinghe County, Xinjiang, China from 1990 to 2014 based on landscape patterns and spatial statistics. *Environ. Earth Sci.* **2018**, *77*, 491. [CrossRef]
41. Peng, J.; Wang, Y.; Ye, M.; Wu, J.; Zhang, Y. Effects of land-use categorization on landscape metrics: A case study in urban landscape of Shenzhen, China. *Int. J. Remote Sens.* **2007**, *28*, 4877–4895. [CrossRef]
42. Ren Cang, B.U.; Man, H.Y.; Yu, C.; Zhen, L.X.; He, H.S. A correlation analysis on landscape metrics. *Acta Ecol. Sin.* **2005**, *25*, 2764–2775.
43. McGarigal, K.; Cushman, S.; Neel, M.; Ene, E. FRAGSTATS: Spatial Pattern Analysis Program for Categorical Maps. Computer software program produced by the authors at the University of Massachusetts, Amherst. 2012. Available online: http://www.umass.edu/landeco/research/fragstats/fragstats.html. (accessed on 6 February 2019).
44. Turner, M.G.; Gardner, R.H.; O'Neill, R.V. Landscape ecology in theory and practice. *Geography* **2003**, *83*, 479–494.
45. Wu, J. *Landscape Ecology: Pattern, Process, Scale and Hierarchy*; High Education Press: Beijing, China, 2000; p. 258.
46. Bojie, F.U.; Liang, D.; Nan, L.U. Landscape ecology: Coupling of pattern, process, and scale. *Chin. Geogr. Sci.* **2011**, *21*, 385–391.
47. Fang, S.; Zhao, Y.; Han, L.; Ma, C. Analysis of landscape patterns of arid valleys in China, based on grain size effect. *Sustainability* **2017**, *9*, 2263. [CrossRef]
48. Wu, W.; Fan, S.; Xu, L.; Zhang, M.; Ou, M. Grain size effect of landscape metrics in Wuxi City. *J. Nat. Resour.* **2016**, *31*, 413–424.
49. Sun, Y.; Sun, Z.; Zhang, J.; Zhang, L.; Meng, Q. *Assessing the Impacts of Grain Sizes on Landscape Pattern of Urban Green Space*; SPIE: Bellingham, WA, USA, 2017; p. 186.
50. Teng, M.; Zeng, L.; Zhou, Z.; Wang, P.; Xiao, W.; Dian, Y. Responses of landscape metrics to altering grain size in the Three Gorges Reservoir landscape in China. *Environ. Earth Sci.* **2016**, *75*, 1055. [CrossRef]
51. Gomarasca, M.A. *Land Use/Land Cover Classification Systems*; Springer: Dordrecht, The Netherlands, 2009. [CrossRef]
52. Zhao, Y.; Murayama, Y. *Effect of Spatial Scale on Urban Land-Use Pattern Analysis*; Springer: Dordrecht, The Netherlands, 2011.
53. Zhou, S.; Che, T.; Dai, L. Based on the type of ground site representative of snow remote sensing products precision evaluation. *Remote Sens. Technol. Appl.* **2017**, *32*, 228–237.